



HAL
open science

The Potential Scope of the Ultrasonic Surface Reflection Method Towards Mechanical Characterisation of Isotropic Materials. Part 2. Experimental Results

Violaine Tinard, Pierre Francois, Christophe Fond

► To cite this version:

Violaine Tinard, Pierre Francois, Christophe Fond. The Potential Scope of the Ultrasonic Surface Reflection Method Towards Mechanical Characterisation of Isotropic Materials. Part 2. Experimental Results. *Experimental Mechanics*, 2021, <10.1007/s11340-021-00731-8>. <hal-03412189>

HAL Id: hal-03412189

<https://hal.science/hal-03412189v1>

Submitted on 2 Nov 2021

HAL is a multi-disciplinary open access archive for the deposit and dissemination of scientific research documents, whether they are published or not. The documents may come from teaching and research institutions in France or abroad, or from public or private research centers.

L'archive ouverte pluridisciplinaire **HAL**, est destinée au dépôt et à la diffusion de documents scientifiques de niveau recherche, publiés ou non, émanant des établissements d'enseignement et de recherche français ou étrangers, des laboratoires publics ou privés.



HAL Authorization

The potential scope of the ultrasonic surface reflection method towards mechanical characterisation of isotropic materials. Part 2. Experimental results

V. Tinard^a (corresponding author, e-mail: vtinard@unistra.fr, phone: +33 (0)368858739, fax: +33 (0)368858608)

P. François^a (pierre.francois@unistra.fr)

C. Fond^a (christophe.fond@unistra.fr)

^a ICube, Université de Strasbourg, CNRS UMR 7357, 300 bd Sébastien Brant - CS 10413 - F-67412 ILLKIRCH Cedex, FRANCE

AUTHORS CONTRIBUTION

All authors contributed to the study conception and design. Material preparation, data collection and analysis were performed by Violaine Tinard, Pierre François and Christophe Fond. The first draft of the manuscript was written by Violaine Tinard and all authors commented on previous versions of the manuscript. All authors read and approved the final manuscript.

KEYWORDS

Ultrasonic methods, Surface Reflection Method, Viscoelasticity, Elastomer.

ABSTRACT

Background: This paper is Part 2 of a study on the scope of the ultrasonic Surface Reflection Method (SRM). Part 1 deals with the theoretical conditions for a satisfactory usage of this method. **Objective:** This second part validates the practical feasibility and reliability of the SRM method by comparison with the conventional Transmission Method (TM) in cases where the latter is applicable. **Methods:** Two experimental devices (one for SRM and one for TM) are developed and measurements of shear and bulk moduli are carried out at ultrasonic frequency (610 kHz) and at room temperature. **Results:** The experimental conditions in terms of sample geometry, pulse characteristics and interfacial transmission required to obtain a given accuracy on the measurement are stated. The SRM is then validated against other experimental methods and is used to determine the shear modulus of a carbon black filled neoprene at ambient temperature ($T = 21^{\circ}\text{C}$) and ultrasonic frequency. **Conclusions:** The benefit brought by this method is well demonstrated: a unique measurement allows the determination of all the moduli of a highly damping isotropic material (carbon black filled neoprene) not achievable by other methods.

1. INTRODUCTION

Ultrasounds have been used since a long time to measure the mechanical properties of materials. The most commonly used techniques are the Transmission Method (TM), the Transmission in Water Bath Method (TWBM) and the Pulse-echo method (BRM). These three methods and their respective advantages and limitations are described in detail in Part 1. It has been proved that they do not apply in case of transverse waves in

rubber-like materials due to the too high attenuation [1, 2]. Another existing technique is the Surface Reflexion Method (SRM) that has been first described by Mason et al. [3] and O’Neil [4]. Since, this technique has rarely been applied as it presents difficulties of experimental implementation [5-7]. In the Part 1 of this paper, it has been proved that the SRM can only be applied if the reference material is adapted to the material to be tested and if very high accuracy in the measurement of phase and amplitude of the two waves is obtained.

The present paper describes the experimental conditions in terms of sample geometry, pulse characteristics and interfacial transmission required to obtain a given accuracy on the measurement. The SRM is then validated by comparison with the TM for an elastic material (aluminium) and a viscoelastic material (carbon black filled neoprene). Finally, it is used to determine the shear modulus of a carbon black filled neoprene at ambient temperature ($T = 21^{\circ}\text{C}$) and ultrasonic frequency.

2. EXPERIMENTAL SETUPS

Two ultrasonic measurement methods are used in this study. The first one is the traditional TM. The corresponding experimental setup is illustrated in figure 1. Tests are performed on two samples of different thicknesses (L and $2L$) to eliminate the influence of the transmission coefficient at interfaces between the transducers and the material.

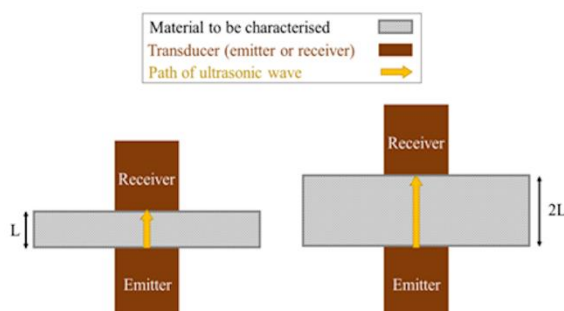


Figure 1. Illustration of the Transmission Method (TM).

Once the tests have been carried out, the ratio of the amplitudes of the two transmitted waves (one for each sample thickness) U is computed using equation 1.

$$U = u_L/u_{2L} \quad \text{Eq. 1}$$

The attenuation value in the material is deduced from the ratio thus obtained and modified by a coefficient taking into account the diffraction phenomenon (see section 3.2.).

$$\alpha = -\frac{1}{L} \ln \left(\frac{U}{\beta} \right) \text{ with } \begin{cases} \beta = 1 \text{ in near - field} \\ \beta = 0.5 \text{ in far - field} \end{cases} \quad \text{Eq. 2}$$

The phase celerity of the transmitted waves is also determined according to the usual formula:

$$c = L/\Delta t \quad \text{Eq. 3}$$

with Δt the difference of transit times between the two thicknesses.

The values of α and c are then used to calculate the desired measurands (either P-wave moduli M' and M'' or shear moduli G' and G'') according to equation 6 of Part 1.

The second ultrasonic method used here is the SRM that is illustrated in figure 2. This method is based on the measurement of the ratio of the amplitude of the reflected wave at the interface between two materials to the amplitude at the air interface. The two materials are bonded together by means of cyanoacrylate glue under a loading of 40 kPa. The glue thickness obtained can be considered negligible (typically less than 0.03 mm) in front of the longitudinal and transverse wavelengths at 610 kHz ($\lambda_l = 4.4$ mm and $\lambda_t = 2.3$ mm).

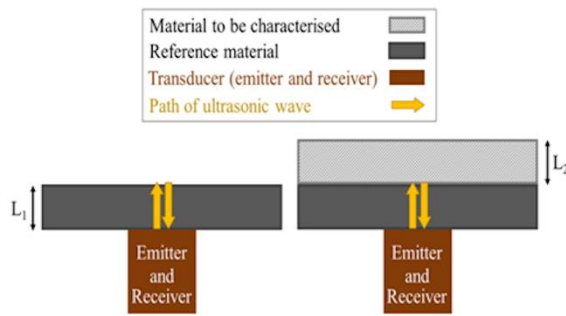


Figure 2. Illustration of the Surface Reflection Method (SRM).

A longitudinal wave transducer (V 189-RB, 38.1 mm active diameter, 610 kHz central frequency, Olympus Corporation, Tokyo, Japan) and a shear wave transducer (V 151-RB, 25.4 mm active diameter, 610 kHz central frequency, Olympus Corporation, Tokyo, Japan) were used to perform the experiments. A PXIe-1073 waveform generator card (National Instruments, Austin, Texas, USA) produced an electrical signal transferred to the transducers. The received signal was averaged over 200 bursts to enhance the signal-to-noise ratio. A LabVIEW® script allowed to control the ultrasonic measurements.

The formulas for determining measurands are detailed in Part 1 of this article (section 2.2.2. equation 15). For both methods, the amplitude, phase and actual frequency values are obtained by performing a Hilbert transform on the raw signal (see section 4.2.).

The coupling between the transducer and the sample is traditionally performed by means of a couplant, the effect of which must be taken into account in the measurements. The couplant thickness has a significant effect on the value of the amplitude and phase of the transmitted wave. It is therefore imperative to perform echo measurements on air and on the material to be characterised under conditions of

identical couplant thicknesses. However, it is difficult to control the initial couplant thickness. To ensure that measurements are always made under similar conditions, a pressure of 80 kPa is exerted for 12 hours on the transducer after mounting the device (see figure 3). This time of 12 hours was determined from the flow equation of the couplant (incompressible Newtonian fluid) between the transducer and the sample and prior measurement of its viscosity ($\mu = 835 \text{ Pa}\cdot\text{s}$).

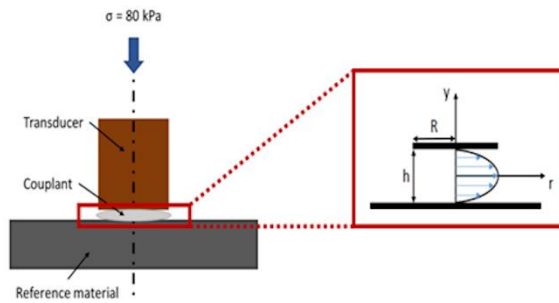


Figure 3. Illustration of the setting up of the couplant.

According to Leider & Bird [8], the relation between the mean pressure exerted on the couplant and its thickness h is:

$$\langle P \rangle = -\frac{3\mu R^2}{2h^3} \frac{dh}{dt} \quad \text{Eq. 4}$$

Where μ represents the Newtonian viscosity.

Solving equation 4 gives the evolution of the couplant thickness as a function of time, with the initial thickness h_0 as a parameter.

$$h(t) = \frac{1}{\sqrt{2\kappa t + \frac{1}{h_0^2}}}, \text{ where } \kappa = \frac{2\langle P \rangle}{3\mu R^2} \quad \text{Eq. 5}$$

Figure 4 below considers four possible initial couplant thicknesses and presents their evolution over time. The results indicate that it takes a minimum of 10 hours for the

initial coupling thickness to no longer have an influence: after this waiting time, the obtained couplant thickness is identical whatever the initial conditions are.

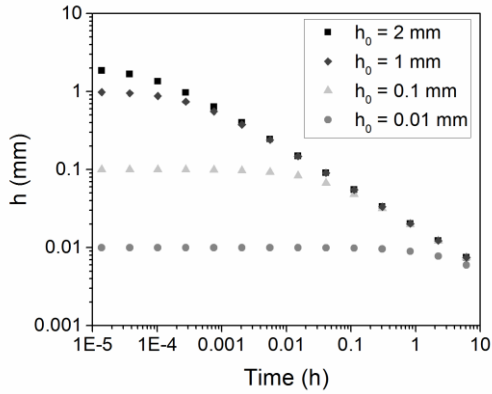


Figure 4. Time evolution of the couplant thickness for various initial thicknesses.

3. SETTINGS

3.1. Choice of reference material

The first part of this paper determines the reference material's mechanical characteristics to obtain a given error margin (typically 10% error on measurands when considering a 1% error on the amplitude measurement). Part 1 indicates that the moduli ratio of the acoustic impedances of the two materials in contact has to be close, typically in the 0.6 to 1.6 range. In addition, this reference material must not be too damping in order to reduce attenuation in the medium, thus preserving a sufficient signal amplitude. Given these conditions, different types of materials are considered in order to determine the most relevant one in the case at stake here, i.e. coupling with neoprene.

Different types of materials are considered as potential reference materials: metals, glass or polymers. The acoustic properties of the selected materials are presented in table 1.

Table 1. Ultrasonic wave celerities of possible materials as reference material at ambient temperature.

Material	ρ (kg.m ⁻³)	c_p (m.s ⁻¹)	c_s (m.s ⁻¹)	Reference
Aluminium	2700	6260	3100	[9]
Glass	2500	5770	3392	[10]
Brass	8500	4430	2120	[11]
Steel	7800	5920	3280	[11]
PMMA	1180	2700	1125	[11]
PEEK	1285	2536	1086	[12]
PVC	1380	2350	1138	[13]

Since there are no values in the literature for the shear wave celerity in neoprene, it was necessary to rely on the properties of a similar material (such as NBR) in order to obtain an order of magnitude of the acoustic impedance of neoprene and thus determine the most relevant reference material. Values found in the literature are presented in table 2.

Table 2. Ultrasonic wave celerities and attenuation coefficients of material similar to neoprene for a frequency of 2 MHz at T = 21°C (extrapolated from Nolle [14]).

Material	ρ (kg.m ⁻³)	c_p (m.s ⁻¹)	α_p (Np.m ⁻¹)	c_s (m.s ⁻¹)	α_s (Np.m ⁻¹)
NBR	1060	2000	368	1000	3300

In the case of a progressive plane wave, the acoustic impedance is determined by equation 6 (from equations 6 and 8 in Part 1). Attenuation is assumed to be negligible for reference materials.

$$|Z^*| = \frac{c * \rho}{\sqrt{1 + \left(\frac{\alpha c}{\omega}\right)^2}} \quad \text{Eq. 6}$$

Figure 5 represents the impedance moduli ratios of the two materials considered (potential reference material and rubber-like material). The obtained results show that metals and glass are not suitable as reference materials since their ratios are not in the optimal range between 0.6 and 1.6. Note that in Mason [3] and O'Neil's study [4], the reference material is fused quartz (glass-like material), which explains their choice to use oblique incidence to increase the accuracy of the measurement.

On the other hand, some polymers considered (PMMA, PEEK and PVC) all have ratios in the optimal zone. The final choice of reference material is PMMA, as this material is available, inexpensive and above all transparent. Fortunately, this transparency allows a first visual verification of the quality of the bonding between the reference material and the material to be tested.

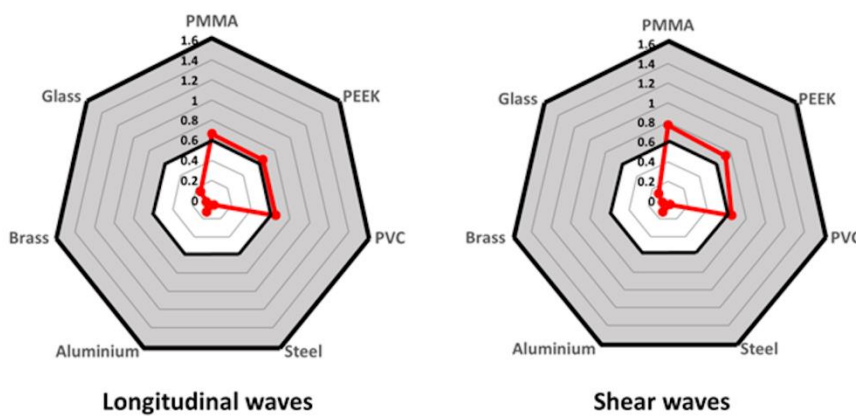


Figure 5. Impedance moduli ratio between rubberlike material and reference materials at ambient temperature. The grey area represents the range of impedance ratios required.

3.2. Practical conditions

It has been shown that, in order to be applied, SRM requires a very high measurement accuracy on the amplitude and phase of the reflected wave in permanent regime.

Although TM is less sensitive to measurement accuracy (see Part 1), the same approach to sample sizing has been adopted for both methods. To achieve this high accuracy requirement, the number of periods of the emitted wave train and the dimensions of the samples for reference material and material to be characterised need to be precisely specified.

In a first step, the minimum number of periods of the emitted wave train will be estimated. As indicated in Part 1 of this paper, the resolution of the wave propagation equation in a continuous medium is carried out by considering the steady state regime reached. Nevertheless, the exact solution of the equation for viscoelastic materials has a transient term. Hence, the amplitude and phase of the reflected wave have to be determined after the transient term has become negligible in comparison with the steady state.

The ratio between the transient term and the amplitude of the steady state is given by equation 7 at given pulsation ω and at a given relaxation time τ (see Appendice for details).

$$\gamma(t) = \frac{\exp(-\omega t/r)}{\sqrt{1+r^2}} \quad \text{with } r = \omega\tau \quad \text{Eq. 7}$$

Figure 6 represents the evolution of γ at a given number of periods of the emitted wave train in function of r .

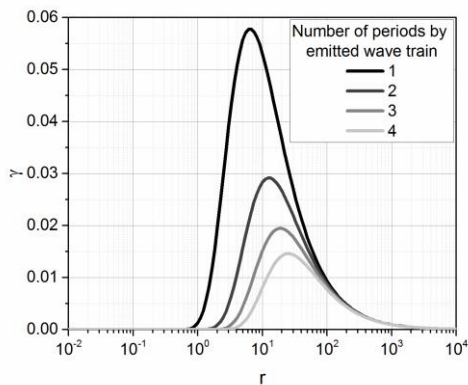


Figure 6. Evolution of γ at a given number of periods of the emitted wave train in function of r

It has been considered that, in the worst case, the influence of the transient term does not distort the measure of the steady state below 2%. This condition is reached for an emitted wave train containing three periods and, at least, one additional period has to be appended for amplitude and phase estimation. Thus, a minimum of four periods is required to achieve desired accuracy. According to the effective thicknesses of our samples, it is suggested that the number of periods of the emitted wave train corresponds to the maximum number of periods respecting the conditions of non-overlapping, conditions which are detailed below.

In a second step, the dimensions of the samples will be specified in order to avoid the overlapping of the signal of interest with secondary echoes.

Amongst the most noticeable secondary echoes are:

- The backing echo: all transducers own a backing material through which a backward wave propagates, reflects at the back of the transducer and finally re-reaches the

piezoelectric membrane. This echo changes in amplitude and localisation in function of temperature. Although the amplitude of this echo is weak and is usually neglected, it has to be taken into account if the signal itself is of low amplitude.

- The second echo corresponds to two travels forward and back through the reference material.
- The pressure wave echoes when using a shear wave transducer: all shear wave transducers emit a non-negligible fraction of pressure wave.
- The bottom echoes: the wave transmitted at the interface reflects at the back of the tested material.
- The potential conversions at the interface between the two materials: longitudinal waves may be partially converted into transverse waves due to interfacial roughness or/and to unplanarity of the incident wave.

The conditions on the transit time of interest in function of the others characteristic times for the two considered methods (TM and SRM) are respectively summarised in tables 3 and 4. The minimum sample thicknesses for a frequency of 610 kHz complying with all non-overlapping conditions for the two methods under consideration is synthesised in table 5.

Table 3. Conditions on the transit time of interest in function of the others characteristic times for TM.

Type of echo	Non-overlapping condition
Second echo	$t_{ml} > t_e$ or $t_{ms} > t_e$
Pressure echo (for shear waves)	$t_{mt} - t_{ml} > t_e$

- t_m is the transit time of the first echo:
 - Subscripts l and t respectively refer to longitudinal and transverse waves
 - Subscripts 1 and 2 respectively refer to reference material and material to be characterised
- t_t is the transit time of the backing echo
- t_e is the pulse duration

Table 4. Conditions on the transit time of interest in function of the others characteristic times for SRM.

Type of echo	Non-overlapping condition
Backing echo	$t_{m,1} > t_t + t_e$
Second echo	$t_{m,1} > t_e$
Pressure echo (for shear waves)	$t_{mt,1} - t_{ml,1} > t_e$
Bottom echo	$t_{ml,2} > t_e$
Conversion echo	$t_{mt,1} - t_{ml,1} > 2t_e$

Table 5. Minimum sample thicknesses for a frequency of 610 kHz complying with all non-overlapping conditions for the two methods under consideration.

Material	Thickness for SRM	Thickness for TM
PMMA	$L_1 > 1,8 \text{ cm}$	$L > 1 \text{ cm}$
Aluminium	$L_2 > 2 \text{ cm}$	$L > 2 \text{ cm}$
Neoprene	$L_2 > 0,6 \text{ cm}$	$L > 0,6 \text{ cm}$

The last aspect for dimensioning the samples is the shape of the beam emitted by the transducer according to the Rayleigh diffraction theory. In the near-field, the mean wave intensity is constant. At the contrary, in the far-field, the intensity decreases with the square of the distance to the transducer, which has to be taken into account for the determination of the attenuation coefficient in TM. Near-field lengths x_c for the three considered materials at a frequency of 610 kHz are given in table 6.

Table 6. Near-field lengths for the three considered materials (frequency of 610 kHz).

Material	Longitudinal wave	Shear wave
PMMA	$x_c = 8 \text{ cm}$	$x_c = 7 \text{ cm}$
Aluminium	$x_c = 3,5 \text{ cm}$	$x_c = 3 \text{ cm}$
Neoprene	$x_c = 11,5 \text{ cm}$	$x_c = 11 \text{ cm}$

Taking into consideration the values in tables 5 and 6, the final sample thicknesses are presented in table 7. For the sake of simplicity, the two sample thicknesses required for TM are in near-field for PMMA and neoprene, and in far-field for aluminium, the conditions of minimum thickness and near-field length being incompatible.

Table 7. Effective sample thicknesses for a frequency of 610 kHz.

Material	Thickness for SRM	Thickness for TM
PMMA	$L_1 = 5 \text{ cm}$	$L = 1,5 \text{ cm}$
Aluminium	$L_2 = 4,5 \text{ cm}$	$L = 4,5 \text{ cm}$
Neoprene	$L_2 = 1,5 \text{ cm}$	$L = 1,5 \text{ cm}$

4. RESULTS

Tests are performed using ultrasonic pressure and shear transducers. The emission frequency is 610 kHz, which corresponds to the centre frequency of the transducers used. All experiments are carried out at constant temperature ($T = 21 \pm 0.1 \text{ }^\circ\text{C}$).

4.1. Experimental determination of the reference material characteristics

The determination of PMMA characteristics is performed using the TM. Results in terms of celerities and attenuation coefficients for longitudinal and transverse waves are respectively presented in figures 7 and 8. The values obtained are consistent with those found in the literature.

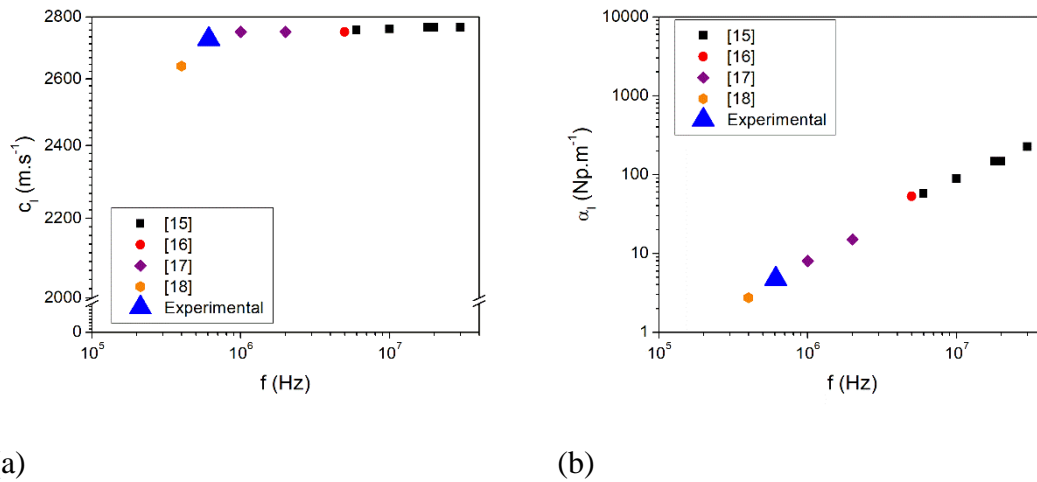


Figure 8. Longitudinal wave celerity (a) and attenuation (b) in PMMA as a function of frequency at room temperature.

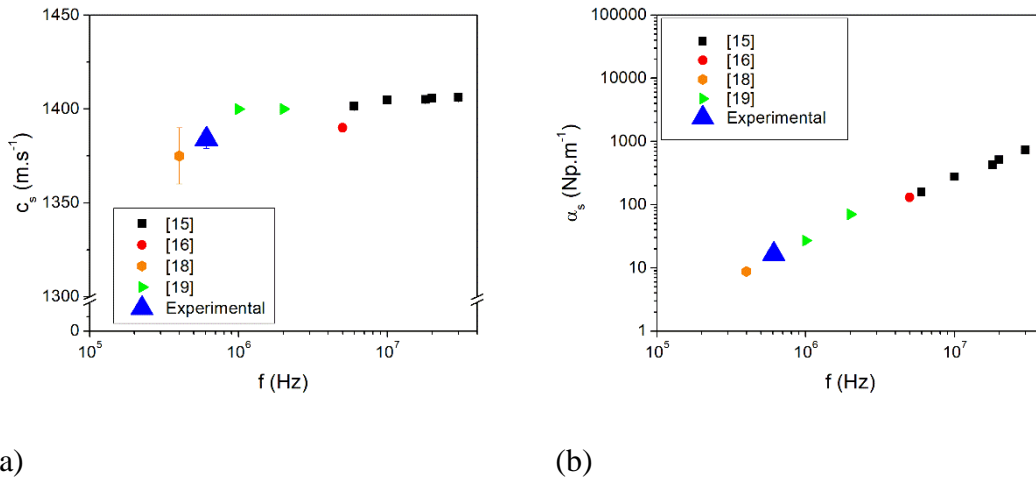


Figure 9. Transverse wave celerity (a) and attenuation (b) in PMMA as a function of frequency at room temperature.

Using equation 6 of Part 1, the values of the various moduli sought are summarised in table 8. The results are compared with values obtained by a non-ultrasonic method based on time-temperature superposition [20].

Table 9. Values of the various moduli for PMMA.

Method	SRM	Broadband Viscoelasticity Spectrometer [20]
G'	2.28 ± 0.08 GPa	1.9 GPa
G''	27 ± 3 MPa	36 MPa
K'	5.8 ± 0.5 GPa	Spectrometer not suitable
K''	24 ± 10 MPa	Spectrometer not suitable
E	6.05 ± 0.25 GPa	Spectrometer not suitable

4.2. Validation

In order to validate the SRM, two types of materials are tested: an elastic material (aluminium) and a viscoelastic material (carbon black filled neoprene). In both cases, the reference material used is PMMA. Two types of ultrasonic waves are used here: longitudinal waves (to determine the P-wave moduli M' and M'') and transverse waves (to determine the shear moduli G' and G''). The experimental values obtained with SRM are compared with those obtained during transmission tests when possible.

The results for aluminium are synthesised in Table 9. The values are consistent for modules M' and G' . It can be noted that the error is higher when using SRM than with TM, which was expected based on the findings in Part 1. For the M'' and G'' modules, the values obtained are no longer meaningful due to the very high error obtained with SRM. Once again, these results were expected since aluminium is an elastic material.

Table 10. P-wave and shear moduli obtained for aluminium with the two considered methods.

Method	M' (GPa)	M'' (GPa)	G' (GPa)	G'' (GPa)
TM	112 ± 1.5	1.37 ± 0.09	26.75 ± 0.24	0.0007 ± 0.007
SRM	120 ± 12	0.72 ± 20	29 ± 3.5	0.34 ± 18.1
[9]	106		26	

The results for neoprene (only for longitudinal waves) are presented in table 10. The values of M' and M'' found with the two methods are consistent and the error obtained with the SRM is, this time, quite acceptable.

Table 11. P-wave moduli obtained for neoprene with the two considered methods.

Method	M' (GPa)	M'' (GPa)
TM	3.95 ± 0.09	0.35 ± 0.02
SRM	4.04 ± 0.23	0.31 ± 0.03

4.2. Determination of the shear mechanical properties of neoprene

After the SRM has been validated, it is applied to determine the shear moduli of carbon black filled neoprene at constant temperature ($T = 21 \pm 0.1$ °C) and at a 610 kHz frequency. The recorded raw signals are provided in figure 9. On this graph, the green frame indicates the time range over which the Hilbert transform of the signals is performed. This transform provides an evaluation of the phase, amplitude and frequency of each signal, as shown in figure 10. As can be seen, the main characteristics of the signals (phase difference, amplitudes and frequencies) are constant over the observation window. Thus, the various moduli are calculated and presented in table 11 in comparison with values from the literature for materials of similar behaviour (computed using master curves based on DMA measurements or based on supersonic wave measurements). The values obtained are of the same order of magnitude as those found in the literature. The differences observed can be explained by the variability of the materials compared as well as frequency and temperature conditions.

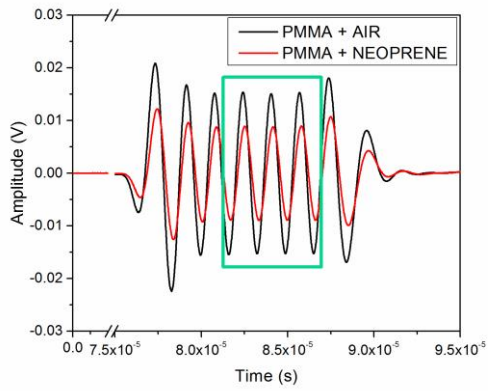


Figure 10. Evolution of the echo's amplitude as a function of time (transverse wave).

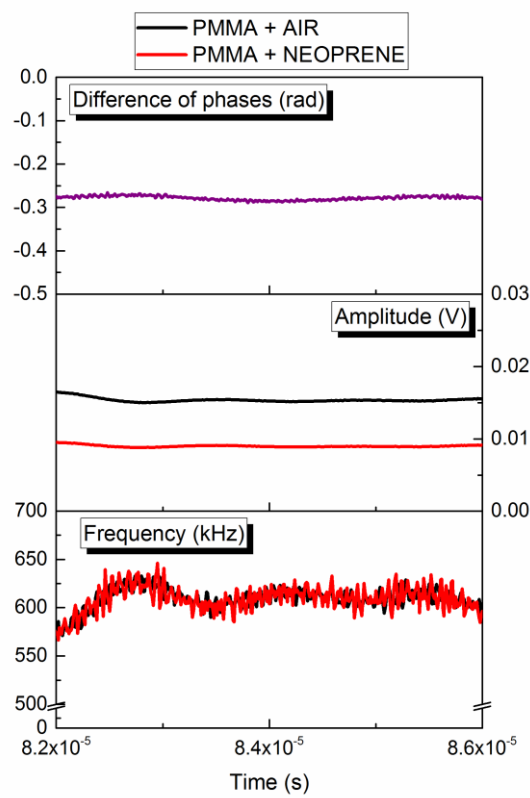


Figure 11. Amplitudes, frequencies and difference of phase of the signal obtained by Hilbert transform.

Table 11. Comparison of values from the literature and obtained experimental values.

Method	SRM	DMA	DMA	DMA	SRM
Reference	This study	[21]	[22]	[23]	[24]
Material	Carbon black filled Neoprene	Carbon black filled (40 phr) Styrene Butadiene Rubber	Carbon black filled (20 phr) Natural Rubber	Silica filled (30 phr) Styrene Butadiene Rubber	Silica filled Styrene Butadiene Rubber
f (kHz)	610	1000	1000	1000	600
T (°C)	21		30	25	
G' (MPa)	121 ± 15	90			
G'' (MPa)	141 ± 10	75			
M' (GPa)	4 ± 0.255				
M'' (MPa)	310 ± 50				
tan(δ) = M''/M'	0.08 ± 0.02				0.08
K' (GPa)	3.88 ± 0.24				
K'' (MPa)	122 ± 40				
E' (MPa)	359 ± 45		219	387	
E'' (MPa)	305 ± 45		227	387	

From these moduli, it is possible to recalculate shear wave celerities and attenuations (see table 12). These values enable us to demonstrate that TM is indeed not suitable for this type of material. The high value obtained for attenuation would imply, for a sample thickness of 1.5 cm, to be able to measure an amplitude ratio of the order of $9e-45$

(equation 2), which is impossible in practice. In order to obtain a measurable amplitude ratio, the thickness of the sample should be of the order of 1 mm. However, this weak thickness introduces other drawbacks. Indeed, as indicated in section 3.2., an emitted wave train with a minimum of three periods is required to reach a steady state regime. In view of the shear wave velocity and frequency considered, this would imply a minimum sample thickness of 2 mm, which is inconsistent with the maximum value of 1 mm found previously.

Table 12. Phase velocity and attenuation obtained during experiments on neoprene for a frequency of 610 kHz at room temperature.

Transverse waves		Longitudinal waves	
c_s (m.s ⁻¹)	α_s (Np.m ⁻¹)	c_p (m.s ⁻¹)	α_p (Np.m ⁻¹)
400 ± 17	6760 ± 495	1698 ± 52	87 ± 16

Moreover, each shear transducer also emits a small fraction of pressure waves (see section 3.2.). For the used transducer, the ratio (experimental value) between the emitted amplitudes of pressure waves and shear waves is 0.03.

Based on the celerity and attenuation values obtained during the tests, it is possible to rebuild the theoretical signal received by a shear transducer (see figure 11) after transit through a one millimetre thick sample. It appears that it is difficult to determine the transit time of the shear wave, since it is drowned in the middle of the pressure wave with, in addition, a much weaker amplitude.

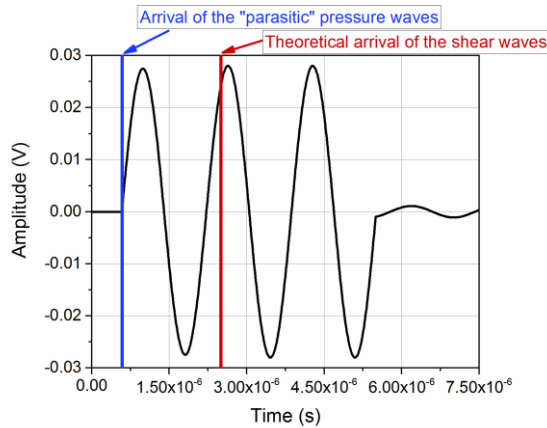


Figure 12. Evolution of the theoretical signal received by a shear transducer after transit through a one millimetre thick sample

5. CONCLUSION

The objective of this study was twofold: on the one hand, to provide all the practical conditions for the implementation of SRM, and on the other hand, to measure the high frequency shear moduli of an elastomer at room temperature.

In order to correctly dimension and configure the measuring system, three physical phenomena have to be considered. Firstly, the duration of the transient phase must be taken into account in the case of a viscoelastic solid: calculations prove that an emitted wave train with three periods is needed to ensure that a quasi steady state regime is reached. Secondly, the sample thicknesses should be chosen so as to avoid the overlapping of the different echoes occurring. Finally, the waiting time and the load applied to the couplant must be such that a reproducible couplant thickness can be obtained regardless of its initial thickness. This analysis of the optimal conditions for the application of the SRM allowed measurements to be performed with satisfactory

accuracy. It appears that SRM can be used to determine all the modules of a highly damping isotropic material.

ACKNOWLEDGMENT

The authors wish to thank: P. Wolff from the University of Strasbourg for helping during the experimental developments, Pascale Lenig-Santoro for providing language help, Demathieu et Bard industry for their financial support, the National Center for Scientific Research (CNRS) for their financial support, the Robert Schuman Institute of Technology, part of the University of Strasbourg for kindly hosting the experiments and making available their experimental devices and, as well, for their financial support.

This is a preprint of an article published in *Experimental Mechanics*. The final authenticated version is available online at: <https://doi.org/10.1007/s11340-021-00731-8>.

ETHICAL STATEMENT / CONFLICT OF INTEREST

All authors certify that they have no affiliations with or involvement in any organization or entity with any financial interest or non-financial interest in the subject matter or materials discussed in this manuscript.

APPENDIX

The duration of the transient term is equivalent to the relaxation time of the viscoelastic material. It is well known that for polymer materials it exists a large range of relaxation times and in consequence a large range of transient term durations. A generalized

Maxwell model often represents this behaviour. Let us consider the i^{th} branch of the Maxwell model, the associated stress is solution of equation A.1:

$$\sigma_i = D_i e^{-\frac{t}{\tau_i}} \int_{-\infty}^t e^{\frac{t'}{\tau_i}} \frac{d\varepsilon}{dt'} dt' \quad \text{Equation A.1}$$

Where $\tau_i = \frac{\eta_i}{D_i}$, η_i , ε and D_i respectively represents the relaxation time, the viscosity, the deformation and the associated modulus of the i^{th} branch.

Considering a sinusoidal deformation starting at $t=0$, the solution of equation A.1 is:

$$\sigma_i = D_i \left(\underbrace{\frac{r^2}{1+r^2} \sin(\omega t) + \frac{r}{1+r^2} \cos(\omega t)}_{\text{permanent term}} - \underbrace{\frac{r}{1+r^2} e^{-\frac{t}{\tau_i}}}_{\text{transient term}} \right) \quad \text{Equation A.2}$$

With $r = \omega\tau_i$

REFERENCES

- [1] Ferry JD (1980) Viscoelastic properties of polymers. John Wiley & Sons
- [2] Burg EVD, Grill W (2010) Characterization of elastomers with transverse sonic waves. Polym Test 29:281 – 287.
<https://doi.org/10.1016/j.polertesting.2009.12.001>
- [3] Mason WP, Baker WO, McSkimin HJ, Heiss JH (1949) Measurement of shear elasticity and viscosity of liquids at ultrasonic frequencies. Phys Rev 75:936 – 946.
<https://doi.org/10.1103/PhysRev.75.936>
- [4] O’Neil HT (1949) Reflection and refraction of plane shear waves in viscoelastic media. Phys Rev 75:928 – 935. <https://doi.org/10.1103/PhysRev.75.928>
- [5] Alig I, Sulimma J, Tadjbakhsch S (1997) Ultrasonic shear wave reflexion method

- for measurements of the viscoelastic properties of polymer films. *Rev Sci Instrum* 68:1536 – 1542. <https://doi.org/10.1063/1.1147643>
- [6] Yoneda A, Ichibara M Shear viscoelasticity of ultrasonic couplers by broadband reflectivity measurements. *J Appl Phys* 97:2005.
<https://doi.org/10.1063/1.1850180>
- [7] Chang J-J, Li Y-Y, Zeng X-F, et al (2019) Study on the viscoelasticity measurement of materials based on surface reflected waves. *Materials* 12:1875 – 1890. <https://doi.org/10.1063/1.4918787>
- [8] Leider PJ, Bird RB (1974) Squeezing flow between parallel disks. I. Theoretical analysis. *Ind Eng Chem Fundam* 13:336 – 341.
<https://doi.org/10.1021/i160052a007>.
- [9] Kawashima K (1984) Quantitative calculation and measurement of longitudinal and transverse ultrasonic wave pulses in solid. *IEEE Transactions on Sonics and Ultrasonics* 33 – 39. <https://doi.org/10.1109/T-SU.1984.31480>.
- [10] Guyott CCH, Cawley P (1988) The measurement of through thickness plate vibration using a pulses ultrasonic transducer. *J Acoust Soc Am* 83:623 – 631.
<https://doi.org/10.1121/1.396156>
- [11] Sutherland HJ (1978) Acoustical determination of the shear relaxation functions for polymethyl methacrylate and Epon 828Z. *J Appl Phys* 49:3941–3945.
<https://doi.org/10.1063/1.325403>
- [12] Fitch DA, Hoffmeister BK, De Ana J (2010) Ultrasonic evaluation of polyether ether ketone and carbon fiber-reinforced PEEK. *J Mater Sci* 45:3768 – 3777.
<https://doi.org/10.1007/s10853-010-4428-1>
- [13] Afifi HA (2003) Ultrasonic pulse echo studies of the physical properties of

- PMMA, PS, and PVC. *Polym – Plast Technol Eng* 42:193 – 205.
<https://doi.org/10.1081/PPT-120017922>
- [14] Nolle AW, Sieck PW (1952) Longitudinal and transverse ultrasonic waves in a synthetic rubber. *J Appl Phys* 23:888 – 893. <https://doi.org/10.1063/1.1702325>
- [15] Asay JR, Lamberson DL, Guenther AH (1969) Pressure and Temperature dependence of the Acoustic Velocities in Polymethylmethacrylate. *J Appl Phys* 40:1768–1783. <https://doi.org/10.1063/1.1657846>
- [16] Tran HTK, Manh T, Johansen TF, Hoff L (2016) Temperature Effects on Ultrasonic Phase Velocity and Attenuation in Eccosorb and PMMA, in: *IEEE Int. Ultrasonics Symp. Proc* 2016.
- [17] Biwa S, Ito N, Ohno N (2001) Elastic properties of rubber particles in toughened PMMA: ultrasonic and micromechanical evaluation. *Mech Mater* 33:717–728.
[https://doi.org/10.1016/S0167-6636\(01\)00087-4](https://doi.org/10.1016/S0167-6636(01)00087-4)
- [18] Aksoy HG (2016) Broadband ultrasonic spectroscopy for the characterization of viscoelastic materials. *Ultrasonics* 67:168–177.
<https://doi.org/10.1016/j.ultras.2016.01.012>
- [19] Sutherland HJ (1978) Acoustical determination of the shear relaxation functions for polymethyl methacrylate and Epon 828Z. *J Appl Phys* 49:3941–3945.
<https://doi.org/10.1063/1.325403>
- [20] Capodagli J, Lakes R (2008) Isothermal viscoelastic properties of PMMA and LDPE over 11 decades of frequency and time : a test of time-temperature superposition. *Rheologica Acta* 47:777 – 786. <https://doi.org/10.1007/s00397-008-0287-y>.
- [21] Fritzsche J, Klüppel M (2011) Structural dynamics and interfacial properties of

filler-reinforced elastomers. *J Phys: Condensed Matter* 23:1–11.

<https://doi.org/10.1088/0953-8984/23/3/035104>

- [22] Ivaneiko I, Toshchevnikov V, Saphiannikova M, et al (2016) Modeling of dynamic-mechanical behavior of reinforced elastomers using a multiscale approach.

Polymer 82:356–365. <https://doi.org/10.1016/j.polymer.2015.11.039>

- [23] Hao D, Li D (2015) Determination of dynamic mechanical properties of carbon black filled rubbers at wide frequency range using Havriliak-Negami model. *Eur J Mech A/Solids* 53:303–310. <https://doi.org/10.1016/j.euromechsol.2015.06.002>

- [23] Omata N, Suga T, Furusawa H, et al (2006) Viscoelasticity evaluation of rubber by surface reflection of supersonic wave. *Ultrasonics* 44:211–215.

<https://doi.org/10.1016/j.ultras.2006.06.019>